Doctoral School on Engineering Sciences
Università Politecnica delle Marche

Extended summary

Local engineering demand parameters for seismic risk evaluation of low ductility reinforced concrete buildings.

Curriculum: Ingegneria delle strutture e delle infrastrutture

Author

Fabio Freddi

Tutor

Luigino Dezi

Date: 30-January-2012

Abstract. Probabilistic methods to evaluate the seismic vulnerability of reinforced concrete (RC) frames are largely used in the context of performance based design and assessment, often describing the structural response using global engineering demand parameters (EDPs) such as the interstory drift. While such EDPs are able to synthetically describe the structural behavior, the use of intermediate or local parameters of RC frames without seismic detailing can enable a more realistic and thorough description of failure mechanisms for structural vulnerability. This study proposes an optimized methodology for the probabilistic evaluation of seismic demand of low ductility RC frames by exploring a range of intermediate, local and global EDPs, identifying appropriate regression models and comparing performances of different ground motion intensity measures used in the probabilistic analysis. Moreover, a probabilistic methodology for assessing the vulnerability of buildings retrofitted by means of dissipative braces is proposed. The methodology use local EDP in order to develop single component and system fragility curves before and after the retrofit. The proposed approach allows to highlight the possible changes in the most significant collapse modalities before and after the retrofit and to evaluate the effectiveness of the retrofit by taking into account the probabilistic properties of the seismic behavior of the considered systems. A benchmark 2-dimensional reinforced concrete frame with low ductility capacity is considered as case study. The frame is designed for gravity-loads only and does not comply with modern anti-seismic code requirements. It is retrofitted by introducing elasto-plastic dissipative braces designed for different levels of their target base-shear capacity, following a design method involving the pushover analysis of the bare frame. The obtained results show the effectiveness of the use of component level vulnerability evaluation of low ductility frames, and the effectiveness of the methodology in describing the changes in the performance due to retrofit. The proposed methodology also allows testing the effectiveness of this simplified criterion employed for the design of braces.

Keywords. Buckling Restrained Braces, Fragility Curves, Local engineering demand parameters, Reinforced concrete frames, Retrofit, Seismic Risk.

1 Problem statement and objectives

The damage occurred during recent earthquakes in many existing reinforced concrete (RC) buildings designed before the introduction of modern anti-seismic codes has shown that these structures are very vulnerable to the seismic action due to their reduced ductility capacity. This underlines the need to develop retrofit techniques for reducing the vulnerability of existing structures and of reliable tools for assessing the effectiveness of the retrofit and the resulting structural safety.

Performance Based Earthquake Engineering (PBEE) [13][34] has gained momentum to support seismic risk mitigation decision-making by disaggregating individual elements of the risk assessment framework. Seismic fragility analysis is a key element of this process used to evaluate the performance of structures under earthquake events based on quantification of structural capacity limits and seismic demand. Probabilistic Seismic Demand Models (PSDMs) are often used to characterize the variation in demand on structures under seismic loading by providing a relationship between structural response and ground motion Intensity Measure (IM). The result of the fragility analysis are fragility curves that provide the probability of exceeding a specified limit state or failure condition, conditional to the strong-motion shaking severity, quantified by means of an appropriately selected IM.

In this context, fragility curves were employed by [25] to investigate the effectiveness of the addition of shear walls, column jacketing, and the confinement of column plastic hinge regions using externally bonded steel plates in reducing the seismic fragility of a existing RC building. In [41] the authors also assessed the effect of column strengthening on the seismic vulnerability of RC frames designed for gravity loads only by comparing the fragility curves of a benchmark building before and after retrofit. Only few works however analyzed the impact of the use of braces on the fragility of existing RC frames. Among these, in [22] the case of viscous dampers is considered, while in [35] and [23] the cases of elastic steel eccentric braces and buckling restrained braces are illustrated respectively. Although these studies have employed probabilistic methodologies for evaluating the effectiveness of different retrofit schemes, some modifications and extensions to these methodologies should be introduced in order to properly address the specific issues deriving from the use of dissipative braces for the retrofit of existing low-ductile RC frames.

The first issue is related to the choice of appropriate engineering demand parameters (EDPs) for monitoring the seismic response and evaluating the performance of the frame and of the retrofit system. In the studies listed above the fragility curves are developed by using the peak inter-storey drift as unique global EDP. This strategy is commonly pursued since monitoring the time-history of the local response of all structural members may be cumbersome, especially when complex models with a high number of degrees of freedoms are considered. The use of this EDP may be adequate to describe the seismic response of ductile frame designed by strength hierarchy rules, but may lead to a high approximation in the vulnerability evaluation and consequently in loss estimates of low ductility frames, since in this case there is not direct relation between local failure mechanism and global interstory drifts. To obtain a more thorough characterization of the vulnerability of the structure, a multi-component fragility study is necessary, as suggested by [5][20].

The system capacity is defined in the studies above based on one of the two approaches: *i)* by assuming the inter-storey drift limits suggested in seismic codes such as [19], or *ii)* by deriving the inter-storey drift limits from the member-level limits suggested in seismic codes (i.e. maximum plastic rotation of members) through a simplified analysis, such as pushover analysis. Obviously, in both the cases, the capacity limits must be properly updated to account for the retrofit, as done in [25] and [41]. Although the first of the two approaches above described is widely and correctly used for new ductile structures thanks to the well-established relations between local failures and global EDPs, it may constitute a serious drawback for the case of existing low-ductile structures for which these relations may differ case by case. Moreover, in the author opinion, this approach cannot be applied, at least at the present knowledge level, to the case of existing low-ductile structures retrofitted by means of dissipative braces for which the relations between local and global demand parameters often change by increasing the retrofit level, due to some specific problems, such as the reduction of the flexural ductility capacity of the columns adjacent to the braces due to the increased compressive forces resulting from the braces action.

With regard to the second approach above described, in addition to being more complex since a pushover analysis must be performed for each analyzed case, it inherits the limits of accuracy affecting the pushover analysis and cannot be followed in some cases, e.g. when dissipative braces with viscous behavior are used, or when the vulnerability of the retrofit system is affected by low cycle fatigue issues. On the other hand, the use of component-specific EDPs [27][31][32][45], such as the strain demand at the most critical element sections or the shear demand on a beam-column joint, though more cumbersome, is not affected by any of the above mentioned limitations. In addition, it permits to appropriately assess in probabilistic terms the performance of the single resisting components (including the braces), their contribution to the system vulnerability and the impact of the retrofit on the local response of the individual members [37]. This aspect may be also crucial for the estimation of the direct costs due to seismic damage, since it is easier to associate a cost to the damage of the single component (beam, column, brace) rather than to the system [20][39].

In addition to the problems deriving from the use of global EDPs, a second relevant issue concerns the evaluation of the retrofit technique effectiveness, which was usually done in the above cited studies by comparing the fragility curves of the structure before and after the retrofit. In fact, when the natural period of the bare frame differs from the natural period of the retrofitted frame, the comparison between fragility curves obtained by using a structure-specific *IM*, such as the spectral acceleration at the fundamental period of the structure, does not directly provide information about the effectiveness of the retrofit. This implied the use of structural-independent IMs for the comparison, such as the less efficient PGA [25]. Furthermore, some synthetic parameters should be used to accurately compute the changes in the safety margin due to retrofit, based not only on the median values of the *IM*, as in [22][35], but also on the dispersion of the fragility, since this parameter also affects the estimate of the seismic risk [9][45].

2 Research Planning and activities

The objective of this study is to investigate the seismic response of low ductility reinforced concrete frames. In particular, use of local Engineering Demand Parameters (EDPs) is proposed in order to give a more complete understanding of the structural behavior of existing RC frames designed without seismic details. Probabilistic Seismic Demand Models (PSDMs) have been proposed and evaluated, and moreover, the retrofit technique based on the use of elasto-plastic braces is considered and its effectiveness is evaluated by a probabilistic methodology based on local EDPs.

In the first part of the study, different EDPs are considered in order to highlight the most significant failure modalities in RC low-ductility frame buildings, optimal PSDMs of single components are developed for various EDPs, and the viability of alternative IMs is explored. In particular PSDMs for local and intermediate EDPs of low ductility RC frames are investigated since they serve as a basis for component level damage and loss assessment. While the form of PSDMs and efficiency of various IMs has been readily explored for global response parameters of RC buildings, this study provides insight into the form of regression model appropriate for such local and intermediate level EDPs as steel and concrete strains, moments and shears on beams and columns, and global responses such as base shear or story accelerations. Furthermore, ground motion IMs are analyzed to identify the IMs that are most appropriate for Probabilistic Seismic Demand Analysis (PSDA) of low ductility RC frames on the basis of such characteristics as IM efficiency and sufficiency. Additionally, the uncertainty about these demand models is assessed including hypothesis tests of the typical lognormal distribution of demands and homoscedasticity assumptions. All the considerations are based on the results of a PSDA performed on a case study. The results of this study provide insight into the form of PSDM, including ideal IM, regression form, and probability distribution, for a range of different demand parameters for low ductility RC buildings. These findings can be used to support the formulation of demand models used in component level fragility analysis and loss estimation conducted within the PBEE framework.

The second part of the study, illustrates a probabilistic methodology for assessing the vulnerability of existing RC buildings with limited ductility capacity retrofitted by means dissipative braces. The methodology use local EDPs in order to develop single component and system fragility curves before and after the retrofit. The proposed approach allows to highlight the possible changes in the most significant collapse modalities before and after the retrofit and to evaluate the effectiveness of the retrofit by taking into account the probabilistic properties of the seismic behavior of the considered systems.

Among the different types of retrofit techniques currently applied, dissipative braces appear to be very promising [10][44]. These braces provide a supplemental path for the earthquake induced horizontal actions and thus enhance the seismic behavior of the frame by adding dissipation capacity and, in some cases, stiffness to the bare frame. It should be noted, however, that the introduction of a bracing system into a low ductility frame often induces remarkable changes both in the collapse modalities and in the probabilistic properties of the seismic response of the structure. The latter aspect assumes a considerable importance in consequence of the high degree of uncertainty affecting the seismic input and of the differences in the propagation of this uncertainty through the two resisting systems (RC frame and dissipative bracing). For these reasons, the evaluation of the effectiveness of this type of retrofit technique in reducing the frame vulnerability should be performed within a probabilistic framework.

The fragility-based methodology proposed in this study overcomes the limits of the studies mentioned in the introduction by combining existing techniques already employed for different structural systems, and tailoring these techniques to the specific problem analyzed. In particular, Incremental Dynamic Analyses (IDA)[47] are performed by subjecting the analyzed system, before and after the retrofit, to a set of natural records scaled in amplitude according to the spectral acceleration at the fundamental period of vibration of the system and local EDPs [27][31][32][45] are chosen to monitor the seismic demand with the aim of capturing the modifications to the frame component response induced by the introduction of the bracing system. Component fragility curves are developed for single structural members (e.g., beam, column or dissipative brace), in order to monitor the most vulnerable elements before and after the retrofit and to highlight the possible changes in the most probable collapse modalities. Moreover, system fragility curves are also developed and synthetically described by only two parameters: the "collapse margin ratio", m_{50} [28], measuring the safety margin with respect to the seismic intensity corresponding to a pre-fixed return period, and the lognormal dispersion β_c, measuring the dispersion of the fragility curve[9]. These two parameters permit to take into account the probabilistic properties of the seismic behavior and capacity of the bare and retrofitted structure and make it possible to compare the performance of the two different systems.

A benchmark RC bi-dimensional frame with limited ductility capacity for which extended experimental results are available [1][7][8] is used as case study for both the parts of the study. The frame has been designed for gravity loads only without any seismic detailing, applying the design rules existing before the introduction of modern anti-seismic codes. In the second part, the frame is retrofitted by inserting a system of buckling-restrained braces (BRBs) with elasto-plastic behavior designed for several levels of the base shear capacity. The braces are designed by applying a widespread method based on the nonlinear static analysis of the bare frame [15][16][26]. The application of the probabilistic methodology permits to evaluate the accuracy of the retrofit design criterion and to draw some important considerations about the changes in the behavior of the system components, the effectiveness of the retrofit and the resulting structural safety.

2.1 Case Study

A three story ordinary moment resisting RC frame which is representative of typical gravity load designed low rise RC frames constructed in the Eastern and Central U.S is adopted as case study. The frame was extensively experimentally investigated by [1][7][8], enabling validation of the finite element model and improved confidence in the global and local dynamic response estimates. This case study has been selected because experimental results concerning local behavior are available allowing an accurate validation of the model in order to achieve reliable results in terms of global and local quantities.

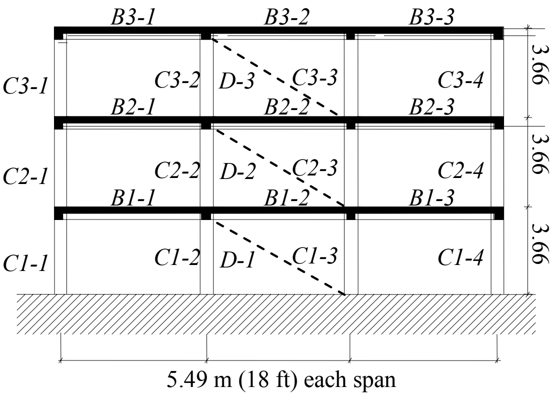

Figure 1. General layout of the structure and braces arrangement (adopted from [7])

The dimension adopted for the frame members are based on a survey of typical construction practices in the Eastern and Central United States conducted by [17]. The frame considered consists of three stories 3.66 m high for a total height of 11 m and three bays, each 5.49 m wide. Columns have a 300×300 mm^2 square section while beams are 230×460 mm^2 at each floor. The provision of [1], Grade 40 steel (f_y = 276 MPa) and concrete with compression resistance f_c' = 24 MPa, were employed in the design. Figure 1 contains the general layout of the structure and complete detailing may be found in [7]. Extended experimental results are available for a 1:3 reduced scale model of the frame and of its subassemblages in [1][7][8]. The experimental results included those obtained during a snap back test, white noise excitation test, shaking table tests of the whole frame [7][8], and quasi-static lateral load tests of columns and beam-column joints subassemblages [1].

In this study a two dimensional Finite Element (FE) model of the structure is developed using OpenSees [33] and employing “Beam with Hinges” elements [42] to model the non-linear behavior of beams and columns. In the plastic hinge zone, the behavior of concrete is described by the Concrete02 material model. The behavior of steel reinforcements is described by the Hysteretic material model and the parameters controlling pinching of force and deformation, damage due to ductility and energy, and degraded unloading stiffness are calibrated to obtain the best fit of the simulated results to the experimental results. The plastic hinge length for both beams and columns was evaluated based on [38]. In order to account of concrete cracking, the elastic part of each element is modeled with an effective flexural stiffness, evaluated through moment-curvature analysis, for the axial force level induced by the dead loads. The rigid-floor diaphragm is modeled by assigning a high value to the axial stiffness of the beams and the masses are deposited at the beam-column connections.

The developed FE model is validated by comparing the available experimental results with the simulated test results of the 1:3 scale numerical FE models of the frame and of its subassemblages. [1] reports the results concerning four 1:3 scale column specimens with and without lap splices loaded with low and high levels of axial forces, representing interior and exterior column at floor slab and beam soffit levels. The columns were subjected to reversed cyclic loading for increasing drift amplitudes up to failure. The study also reports the results of the tests of two 1:3 scale specimens of an exterior and an interior beam-column joint subassemblage, subjected to axial load and reversed cyclic lateral displacements. Figure 2 and Figure 3 show the comparisons between the experimental and the simulated results concerning column specimen 1 (column specimen with lap splices and with low axial load) (Fig. 2a), column specimen 3 (column specimen without lap splices and with low axial load) (Fig. 2b), the interior subassemblage (Fig. 3a) and the exterior subassemblage (Fig. 3b).

The material properties in the 1:3 scaled FE model are defined coherently with experimental test results on the materials specimens. The simulated test results show a satisfactory agreement with the experimental results and demonstrate the capability of the FE model to simulate the cyclic local behavior of the structure. [7] and [8] report the results of the experimental tests carried on the 1:3 scale frame. Snap back and white noise tests were performed to obtain information about the vibration periods and the modal shapes. The first three natural periods measured in the experimental test results (0.538, 0.177 and 0.119 sec) are in close agreement with the periods provided by the 1:3 scale FE model with uncracked gross stiffness properties (0.561, 0.180, and 0.110 sec). A good agreement is also observed in the first three modal shapes.

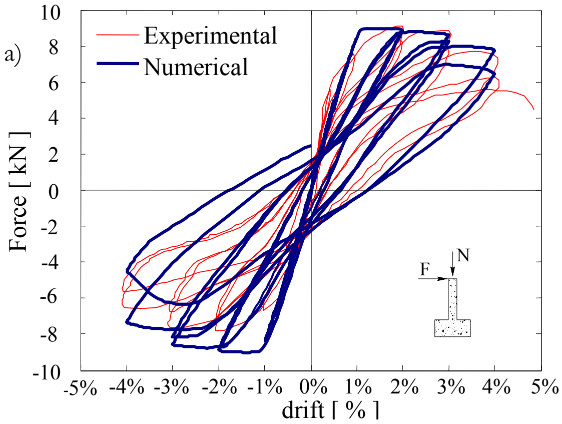

Figure 2. Experimental and numerical lateral load-drift comparison for a) Column specimen 1, b) Column specimen 4.

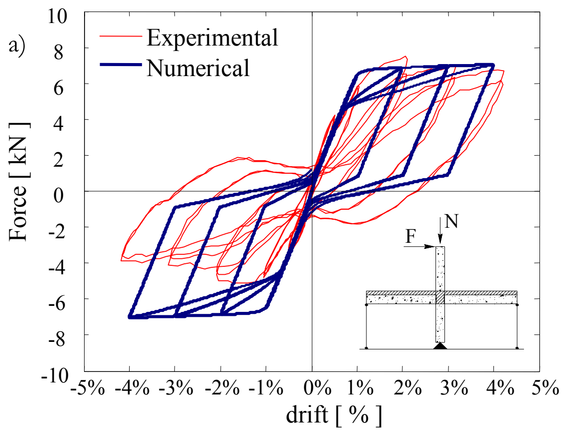

Figure 3. Experimental and numerical lateral load-drift comparison for a) interior slab-beam-column subassemblage, b) exterior slab-beam-column subassemblage.

Shaking table tests were also performed by applying the Kern County 1952, Taft Lincoln School Station, N021E component record scaled for different levels of the seismic intensity (PGA = 0.05g, 0.20g and 0.30g). Figure 4 shows the comparison between the 3rd story displacements of the 1:3 scale experimental and numerical model corresponding to ground motions with PGA of 0.05g (Fig. 4a), 0.20g (Fig. 4b) and 0.30g (Fig. 4c), respectively. In the FE model, damping sources other than the hysteretic dissipation of energy are modeled through the Rayleigh damping matrix, with mass and stiffness related coefficients calibrated such that the values of the damping factor of 3% are obtained for the first two vibration modes. This value provides the best agreement between experimental and simulated results. The agreement between the simulated and experimental response history is quite satisfactory for values of the PGA equal to 0.05g and 0.02g, while for PGA =0.03g the agreement is not as good. However, it should be stressed that only the peak values of the response are of interest for the development of fragility curves and that the simulated peak values are very close to the experimental peak values for all the seismic intensity levels considered.

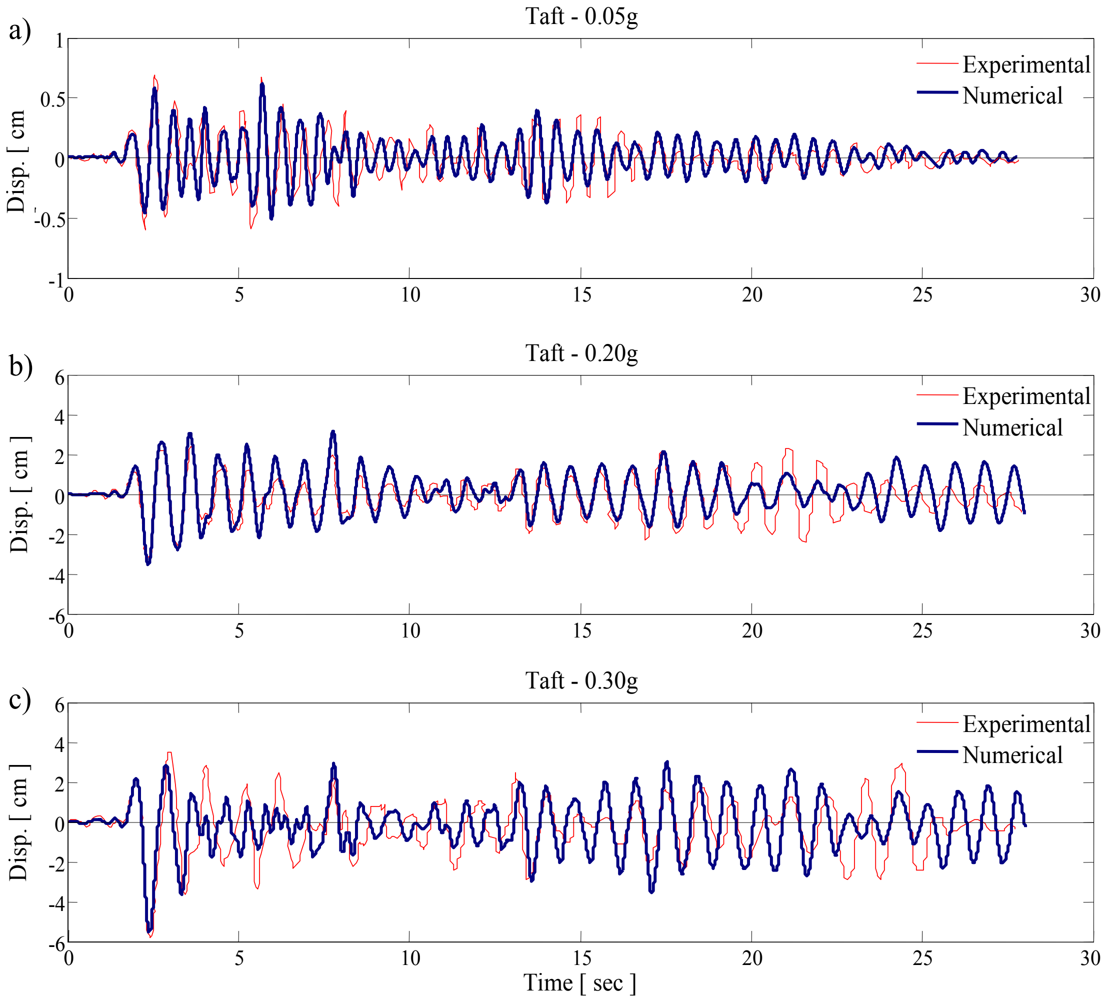

Figure 4. Comparison of dynamic analysis for model validation: a) 3rd story displacement subjected to Taft at PGA of 0.05g, b) 3rd story displacement subjected to Taft at PGA of 0.20g, c) 3rd story displacement subjected to Taft at PGA of 0.30g.

3 Analysis and discussion of the main results

3.1 Optimal PSDMs for low ductility RC frames

The validated finite element model of the prototype structure is used as case study structure to explore the appropriate form of PSDM for low ductility RC frames, including optimal IM and form of regression, amongst other key assumptions for a broad range of EDPs. In particular, the viability of linear versus bilinear regression (in the log-log space) is considered in this study. The ground motion IMs under investigation are shown in Table 1.The IMs considered are chosen among the more popular IMs and other IMs considered easy to use and for which seismic hazard curves are either readily available or computable with a reasonable effort.

Table 1. Intensity Measure

Intensity measure	Description	Units	Range
	Structure Dependent IMs		
S_a	Spectral Acceleration at T_1 (ξ=5%)	g	0.0051 - 0.981
S_v	Spectral Velocity at T_1 (ξ=5%)	cm/sec	1.897 - 204.97
S_d	Spectral Displacement at T_1 (ξ=5%)	cm	0.218 - 42.40
S_{aC}	Sa Predictor [Cordova, 2000][12]	g	0.0013 - 0.259
S_{N1}	Sa Predictor [Lin, 2011][29]	g	0.0013 - 0.281
	Structure Independent IMs		
PGA	Peak Ground Acceleration	g	0.019 - 1.068
PGV	Peak Ground Velocity	cm/sec	1.261 - 130.28
PGD	Peak Ground Displacement	cm	0.188 - 119.70
$S_{a\text{-}02s}$	Spectral Acceleration at 0.2 s (ξ=5%)	g	0.041 - 2.136
$S_{a\text{-}1s}$	Spectral Acceleration at 1 s (ξ=5%)	g	0.0121 - 1.392
I_a	Arias Intensity	cm/sec	1.258 - 928.88
I_v	Velocity Intensity	cm	1.854 - 288.87
CAV	Cumulative Absolute Velocity	cm/sec	113.3 - 3586
CAD	Cumulative Absolute Displacement	cm	6.885 - 639.9

Table 2. Engineering Demand Parameters

EDP	Description	Performance characteristic	Unit
		Local EDPs	
$\varepsilon_{s,max}$	Steel strain	Flexural and Axial behavior	-
$\varepsilon_{c,max}$	Concrete strain	Flexural and Axial behavior	-
ϕ_{max}	Curvature	Flexural behavior	1/m
$\sigma_{j,tens,max}$	Joint tensile stress	Joint behavior	kN/m^2
$\sigma_{j,compr,max}$	Joint Compressive stress	Joint behavior	kN/m^2
		Intermediate EDPs	
V_{max}	Shear	Shear resistance	kN
M_{max}	Moment	Flexural resistance	kNm
		Global EDPs	
$V_{b,max}$	Base Shear	Global behavior	kN
$\Delta_{i,max}$	Story Displacement	Global behavior	m
$\theta_{i,max}$	Interstory Drift	Global and non structural behavior	rad
$St.Vel_{i,max}$	Story Velocity	Global and non structural behavior	m/sec
$St.Acc_{i,max}$	Story Acceleration	Global and non structural behavior	m/sec^2

A set of 240 ground motions from [6] has been used in the nonlinear dynamic analyses, with a range of IM characteristics as indicated in Table 1. The ground motions used in this study are representative of a wide range of variation in terms of source to site distance (from 8.71 to 126.9 km) and soil characteristics with an average shear wave velocity in the top 30 m (V_{s30}) that range from 203 to 2016.1 m/sec while the magnitude of the ground motions range from 5.3 to 7.9. Pulse like ground motions are not included. In order to investigate about all the possible failure modes, 12 EDPs are considered in this study such as shown in Table 2. PSDMs for all the considered IM-EDP pairs are developed by using the dynamic responses from the 240 NTHA in what is often termed a “cloud analysis”. The validated frame model is considered to be deterministic and the variability in local, intermediate, and global responses captured in the PSDA reflects the propagation of ground motion variation alone.

3.1.1 Optimal Regression form

Optimal regression form of PSDMs for response quantities of interest in vulnerability modeling of low ductility RC frames are described as follow. The PSDMs using $S_a(T_1)$ as the IM are shown as an example to explore the regression form, however, all EDP-IM pairs were explored confirming that the behavior in terms of viability of linear versus bilinear regression (in log-log space) is consistent across all IMs. Figure 5 illustrates the PSDMs constructed in the transformed space for four different EDPs, including interstory drifts (θ_I), curvature (ϕ), concrete and steel strains (ε_c and ε_s) for upper section of column C1-1. Similar PSDMs have been developed for all the considered EDPs and for all the critical section of the structure. The results reveal that linear regression of the structural demands relative to $S_a(T_1)$ provides a good fit for the drift, velocity, and acceleration responses while, for local and intermediate EDPs a bilinear regression is indispensable to adequately represent the demand. Bilinear regression of the demand is found to be best fit to build PSDMs reflecting typical stress-strain bilinear behavior of the materials and typical moment-curvature bilinear behavior for sections.

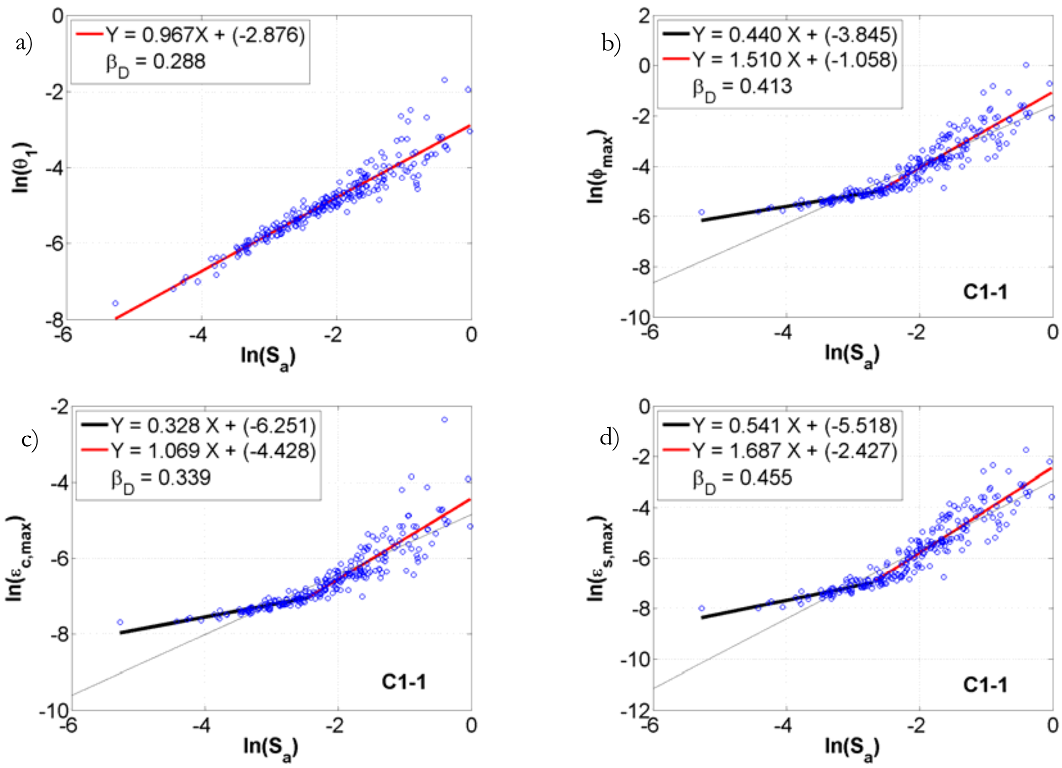

Figure 5. PSDMs comparing linear and bilinear regression for a) Interstory drifts for 1th story, b) Curvature upper section el. C1-1, c) Concrete Strain upper section el. C1-1, d) Steel Strain upper section el. C1-1. $S_a(T_1)$ is used as the IM for illustration.

3.1.2 Intensity measure comparison for different IM

Given the form of regression identified for PSDA of different EDPs a comparison of alternative ground motion IMs is conducted to select the ideal independent variable for the PSDM regression. In order to identify the "best" IM, conditions of practicality, sufficiency, hazard computability and efficiency have to be evaluated. All the IM-EDP pairs evaluated in this study are considered practical and amongst others, the efficiency of an IM is considered as a main decision parameter for IM selection to reduce the uncertainty in the probabilistic seismic demand model. Identification of the "best" IM is challenging since the required conditions may vary for different components even when considering the same EDP (e.g. the dispersion in curvature demands varies across different beams and columns in the structure for a given IM). To facilitate comparison, a statistic of the indicators of each IM properties amongst all components is evaluated for each EDP and IM. The following sections investigate the characteristics of an ideal IM and present the results of the IM comparison.

3.1.2.1 Sufficiency

The IMs from Table 1 are evaluated for sufficiency in terms of conditional statistical independence of the response from magnitude (M) and distance (R) [30][36]. Residuals from the PSDMs, $\varepsilon|IM$, are considered in a linear regression with M and R and hypothesis tests of residual independence from M or R are conducted resulting in p-values [24] used to assess the sufficiency. The sufficiency of each IM is evaluated among all the EDPs and relevant components. Among all of the IM, PGA and $S_{a\text{-}02s}$ are found to be insufficient with respect to magnitude, while PGD, I_v and CAD are found to be insufficient respect to distance. PGV is found to be the best IM that respect the sufficiency hypothesis respect both R and M, while for all the other IMs the sufficiency condition is equally satisfied.

3.1.2.2 Efficiency

Efficiency indicates the amount of variability of an EDP given an IM and can be quantified by the dispersion, $\beta_{D|IM}$ [21]. This estimate of the logarithmic standard deviation ($\beta_{D|IM}$) is calculated from the error of the mathematical demand model with respect to the corresponding realization of the NTHA. Structure dependent IMs tend to be much more efficient for all the considered EDPs relative to the structure independent IMs. Among the structure independent IMs, PGV and $S_{a\text{-}1s}$ are found to be the best while $S_{a\text{-}02s}$ and PGA have the largest dispersions. Among the structure dependent IMs, $S_a(T_1)$ and $S_d(T_1)$ are found to be the best IMs consistent with previously obtained results from studies on framed structures and bridges [43][32]. The dispersions of $S_v(T_1)$, $S_{N1}(T_1)$ and $S_{aC}(T_1)$ are larger, but these IMs are still relatively efficient, in particular with respect to the structure independent IMs. The optimal IM in terms of efficiency does not tend to show dependence upon EDP of interest, and consistent results can be observed looking each EDP independently.

3.1.2.3 Hazard Computability

Among the IMs considered, hazard information is readily available across the United States for PGA, PGV, PGD, and specific spectral quantities corresponding to 0.2 sec and 1.0 sec ($S_{a\text{-}02s}$ and $S_{a\text{-}1s}$), from such entities as the U.S. Geological Survey. For structural dependent IMs considered in this study, hazard curves can be approximated with a reasonable level of effort. While, the definition of hazard curves for other structural independent IMs considered in this study (I_a, I_v, CAD and CAV) is practicable but it requires considerable efforts.

3.1.3 Assessment of the demand variation

This section tests common simplifying assumptions regarding the form of the probabilistic seismic demand model and their validity for a range of EDPs of interest in low ductility RC buildings. In particular, the variation of the dispersion of the demand with increasing ground motion intensity, and its probability distribution, often adopted as lognormal are explored. In order to verify the validity of the widely used homoscedasticity assumption, logarithmic standard deviation values $\beta_{D|IM}$ are defined for different intervals of IM values and in order to verify whether a lognormal distribution of the demand can be assumed, Kolmogorov-Smirnov goodness-of-fit tests are conducted.

3.1.3.1 Homoscedasticity assumption

Homoscedasticity of the demand is often assumed as a simplification of the probabilistic seismic demand model, in which the variation of the demand is considered constant across all IMs and hence a single parameter of the logarithmic standard deviation is adopted to derive fragility curves. In order to verify the validity of the widely used homoscedasticity assumption, the estimates of β_D are calculated for different ranges of the ground motion IM.

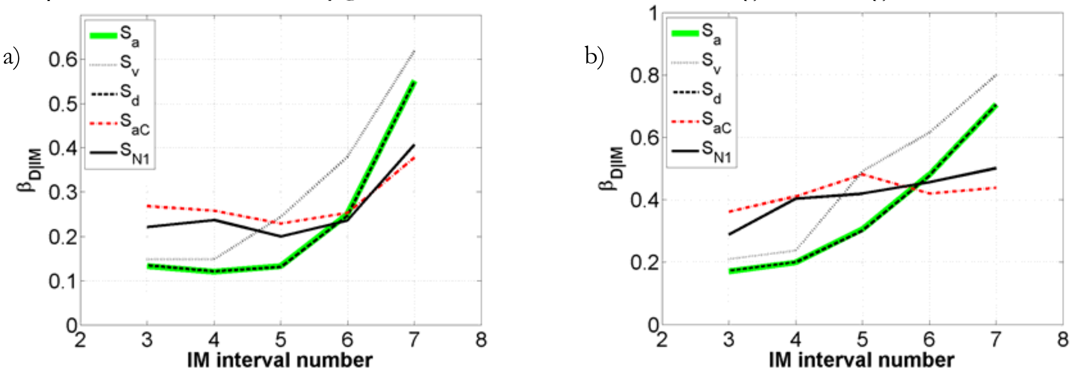

Figure 6. Variation in dispersion of a) Drift at the 1st level of the structure, b) Curvature upper section el. C1-1for the structural dependent IMs.

Figure 6 shows the variation in dispersion for structural dependent IMs for demand models constructed for the interstory drift at the 1st level of the structure and for the for curvature referred to the column C1-1. Results shown that $S_a(T_1)$, $S_d(T_1)$ and $S_v(T_1)$ have a higher variation of dispersion compared with $S_{N1}(T_1)$ and $S_{aC}(T_1)$. This results can be attributed to the fact that for low values of the IM the structural behavior is controlled by the elastic modal period of the structure, while, for higher level events, IMs able to take into account the period elongation caused by inelastic structural behavior are more efficient. Hence, adoption of IMs that account for period elongation (i.e. $S_{aC}(T_1)$ and $S_{N1}(T_1)$) helps to satisfy the homoscedasticity assumption. However, also for these IMs the homoschedasticity assumption is not satisfied. Similar results are found also for other EDPs and other critical sections of the structure. For the structure independent IMs the homoscedasticity assumption is always better satisfied since these IMs are not efficient for all the range of IM values. For global deformational EDPs, such as story displacement and drift, as well as story velocity and story acceleration, the use of $S_{aC}(T_1)$ and $S_{N1}(T_1)$ improves the assumption of an approximately constant value of dispersion. However, the homoscedasticity assumption is never satisfied for local and intermediate EDPs of the RC frame, regardless of IM adopted; it is recommended that the heteroscedasticity instead be considered when assessing the dispersion in probabilistic seismic demand modeling of these IMs.

3.1.3.2 Lognormal distribution assumption

The validity of the typical lognormal probability distribution assumption regarding the variation in demand in PSDAs is investigated through a Kolomogorov-Smirnov goodness-of-fit test [11]. The hypothesis test with a confidence level of 85% is conducted for all of the EDPs considered. The structural dependent IMs tend to produce demand variations that conform to the traditionally assumed lognormal distribution. The percentage failure of the hypothesis test for structural dependent IMs range from 16.5% with $S_d(T_1)$ to 20.8% using $S_{aC}(T_1)$ as the IM. While, for the structural independent IMs this value ranges from 22.3 % with $S_{a\text{-}1s}$ to 34.2 % using $S_{a\text{-}02s}$ as the IM.

3.1.4 Optimal PSDMs results

Optimal PSDMs confirm that linear regression (in the logarithmically transformed space) provides a good fit of the demand for conventionally used global EDPs, while it is found that for local and intermediate EDPs, such as curvature, shear, joint stresses, or material strains, a bilinear regression is required. From the IM study, $S_d(T_1)$ and $S_a(T_1)$ are found to best satisfy the requirement of practicality, sufficiency, hazard computability and efficiency across the range of EDPs, while satisfying traditional lognormal probability distribution assumptions. However, bilinear regressions with heteroscedastic dispersions are required in the PSDA for local and intermediate EDPs, regardless of IM selection.

3.2 Probabilistic methodology for vulnerability assessment

As already mentioned in the introduction, the use of global EDPs permit to drastically reduce the computational effort but, their use may lead to incorrect results in the cases of existing low-ductile structures, since the relations between local and global demand parameters change case by case and among the components. In addition, for the existing low-ductile frames retrofitted using dissipative braces, these relations change by increasing the retrofit level. This is a consequence of some specific problems, such as the reduction of the flexural ductility capacity of the columns adjacent to the braces due to the increased compressive forces induced by the bracing system.

In addition, the use of efficient structure dependent IMs for the evaluation of the retrofit technique effectiveness involves some complications. In fact, when the natural period of the bare frame differs from the natural period of the retrofitted frame, the comparison between fragility curves of the structure before and after the retrofit does not directly provide information about the effectiveness of the retrofit. This implied the use of structural-independent IMs for the comparison, such as the less efficient PGA [25]. Furthermore, some synthetic parameters should be used to accurately compute the changes in the safety margin due to retrofit, based not only on the median values of the *IM*, as in [22][35], but also on the dispersion of the fragility, since this parameter also affects the estimate of the seismic risk [9][45].

This second part of the study illustrates a probabilistic methodology for assessing the vulnerability of existing RC buildings with limited ductility capacity retrofitted by means dissipative braces. Local EDPs are used in order to directly capture the modifications of the frame response and of the capacity induced by the introduction of the bracing system.

The seismic response of the frame before and after retrofit is affected to the uncertainties due to the earthquake input (record-to record variability), the properties defining the system (model parameter uncertainty) and the lack of knowledge (epistemic uncertainty) The effect of model parameters uncertainty and epistemic uncertainty are usually less notable than the effect of record-to-record variability and hence they are not considered in this study. The uncertainty affecting the earthquake input is taken into account by selecting a set of natural ground motion (g.m.) records that reflect the variability in duration, frequency content, and other characteristics of the input expected to act on the system. In particular, records are chosen in a range of magnitude, source to site distance and propagation velocity of *S* waves in the upper 30 m (v_{s30}), so that they are compatible with a uniform hazard spectrum related to a specified soil type. In order to generate fragility curves, Incremental Dynamic Analysis (IDA) [47] is performed by subjecting the system to the selected set of g.m. records for increasing values of the seismic intensity. Based on the results of the first part of the study, spectral acceleration $S_a(T)$ at the fundamental period of the structure T_1 for a damping factor ξ=5% is used as seismic intensity measure IM. This choice requires the scaling of the g.m. records in order to obtain the same value of $S_a(T)$ for the natural period of the structure, which is different for the bare and the retrofitted frames. The result of the multi-record IDAs is a set of samples of appropriately selected EDPs monitoring the system response for discrete values of the IM.

In particular, the local EDPs adopted to monitor the seismic demand on the frame due to flexural and axial forces are the maximum-over-time values of *i)* the concrete compressive strain ε_c and *ii)* the absolute steel strain ε_s at the critical sections of each element (beams and columns) of the frame; moreover the maximum-over-time values of *iii)* the shear force V_s at the critical sections of each element of the frame, *iv)* the diagonal tension stress σ_t and *v)* the diagonal compression stress σ_c at each beam-column joint are recorded in order to monitor the non-ductile mechanisms; finally the maximum-over-time value of *vi)* the damage parameter of each dissipative brace (such as the ductility μ_d for elasto-plastic braces) is also recorded in the retrofitted cases, in order to monitor the demand on the introduced braces. Coherently with the monitored EDPs, the limit states considered to develop the numerical component fragility curves for the bare and the retrofitted frame are: *LS1*) ε_c exceeding the limit ε_{cu} at each element, *LS2*) ε_s exceeding the limit ε_{su} at each element, *LS3*) the shear demand exceeding the shear resistance at each element, *LS4*) σ_c exceeding the resistance in compression $\sigma_{c,u}$ at each joint, *LS5*) σ_t exceeding the resistance in tension $\sigma_{t,u}$ at each joint, and *LS6*) the damage parameter overcoming the capacity of each dissipative brace (i.e. the ductility demand μ_d overcoming the ductility capacity μ_{du} at each dissipative brace).

The system fragility curves are developed by comparing the demand with the capacity for all the monitored components and by assuming a series arrangement of the components, i.e. failure in one component yields system failure. It is noteworthy that the series arrangement represents the situation in which all the monitored limit states are required to be satisfied. Consequently, if not premature failure of the non ductile mechanisms occur, the first flexural failure of the most critical section of the frame is assumed as the system failure. It is evident that the bare frame has residual resources after the first failure but, in order to limit damages on the bare frame elements, they are not considered in the retrofit. Hence, the system failure is assumed coincident with the first flexural failure of the most critical section of the frame or the first failure of the most critical brace. The comparison between the system and the single component fragility curves permits to quickly evaluate the most vulnerable components before and after the retrofit and their contribution to the system vulnerability. Moreover, the comparison between the vulnerabilities of the frame components and of the dissipative devices permits to evaluate the reliability of the simplified design method adopted. The fragility points obtained through the numerical procedure are fitted by two-parameters cumulative lognormal distribution functions [14], whose parameters have been obtained by least-square minimization. Finally, the system fragility curves obtained are synthetically described by the two following parameters: the median IM at collapse, $IM_{c,50}$, i.e. the IM corresponding to 50% probability of failure of the system, and the dispersion measure, β_c, given by:

$$\beta_c = \frac{1}{2}\ln\left(\frac{IM_{c,84}}{IM_{c,16}}\right) \tag{1}$$

where $IM_{c,84}$ and $IM_{c,16}$ are the IM values corresponding to the 84th and the 16th fractiles of the fragility curve. However the first parameter $IM_{c,50}$ does not directly provide information about the effectiveness of the retrofit, since the natural period of the bare frame differs from the natural period of the retrofitted frame. For this reason the so called "*collapse margin ratio*" m_{50} is introduced, defined as the ratio between the $IM_{c,50}$ parameter and the value of the maximum considered earthquake spectral intensity at the system natural period $S_{a,max}(T)$. In this study the maximum considered earthquake spectrum is assumed as the uniform hazard spectrum scaled so that m_{50}=1, i.e. $IM_{c,50} = S_a(T)$, for the bare frame, as illustrated in Figure 7. In this way, by assuming that the spectral shape does not change with the seismic input intensity, this normalized factor of safety directly measures the increment of the seismic intensity that can be withstood by the structure due to retrofit by accounting for the change in the IM due to the variation of the system natural period. In a similar way, based on the ratio $IM_{c,16}/S_{a,max}(T)$ and $IM_{c,84}/S_{a,max}(T)$, the factors m_{16} and m_{84} corresponding to the 16th and 84th fractiles are defined. These parameters are used to compare the performance of the bare and of the retrofitted frame and, thus, to assess in probabilistic terms the effectiveness of the retrofit.

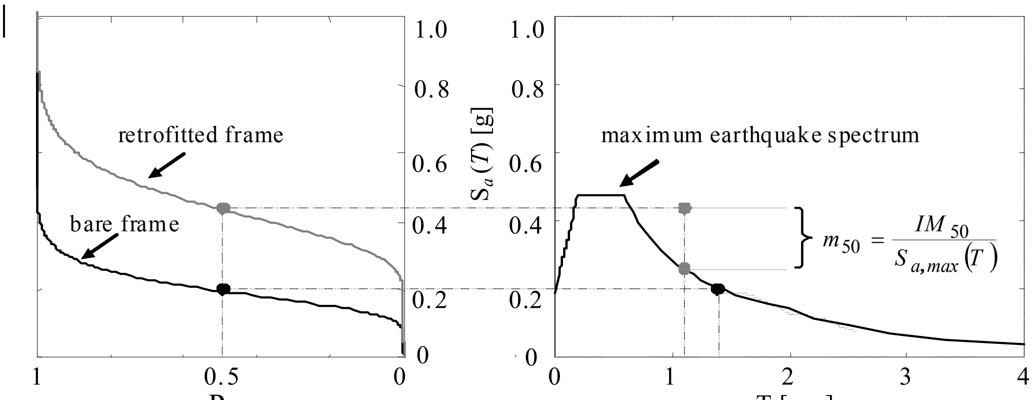

Figure 7. Collapse margin Ratio (m_{50})

3.2.1 Retrofit design methodology

This paragraph synthetically illustrates the procedure employed for the design of the dissipative braces exhibiting an elasto-plastic behavior. The interested reader is referred to [15] for a more detailed description.

The dissipative braces considered in this study are made by an elasto-plastic dissipation device placed in series with an elastic brace exhibiting adequate overstrength. These devices are usually placed in series since they are quite short, so that they are able to yield for small displacements and thus can be used in the retrofit of RC frames with limited ductility which cannot undergo large displacements without failure. The properties of the dissipative brace can be defined based on the properties of its components. In particular, if K_b denotes the axial stiffness of the elastic brace and K_0, F_0 and μ_{0u} respectively the stiffness, yielding force and ductility capacity of the elasto-plastic device, the dissipative brace stiffness K_d and ductility capacity μ_{du} are given by:

$$K_d = \frac{K_b K_0}{K_b + K_0} \quad , \quad \mu_{du} = \frac{K_0 + K_b \mu_{0u}}{K_b + K_0} \tag{2}$$

while the yielding force F_d is equal to F_0. Usually, the value of μ_{0u} is given by the dissipation device manufacturer, while the value of μ_{du} depends on the ratio K_0/K_b and is design parameter which must be chosen at the beginning of the design procedure. It should be observed that large values of the ductility ratio μ_{du} / μ_{0u} lead to very onerous metallic brace dimensions, whereas low values of the ductility ratio lead to small brace dimensions and consequently to brace buckling problems. The method followed for designing the dissipative system is based on pushover analysis of the existing frame under a distribution of forces corresponding to its first vibration mode. The "collapse point" for the frame is defined by the values of the maximum displacement at the top floor d_u and by the maximum base shear V^1_f the frame is capable to withstand without any rupture at the plastic hinges. The dissipative bracing system is assumed to behave as an elastic-perfectly plastic system, with shear capacity equal to V^1_d, ductility capacity equal to μ_{du} and with the same collapse displacement of the bare frame (d_u). This last assumption aims at obtaining a simultaneous failure of both the frame and the dissipative braces. It is noteworthy that the value of V^1_d is a design choice and depends on the objective of the retrofit. For a given value of V^1_d, the stiffness of the bracing system at the first story is given by:

$$K_d^1 = \frac{V_d^1 \mu_{du}}{d_u \delta^1} \tag{3}$$

where δ^1 is the inter-story drift at the first story, normalized with respect to the top floor displacement according to the first modal shape. The shear V^i_d and stiffness K^i_d of the dissipating bracing system at each story can be determined by the following relations:

$$V_d^i = V_d^1 v^i \quad , \quad K_d^i = K_d^1 k^i \tag{4}$$

where v^i and k^i are the shear force and stiffness at each story, normalized with respect to the base shear and base stiffness according to the first mode of the bare frame. By this way, the stiffness distribution of the dissipative braces at each story ensures that the first modal shape of the bare frame remains unvaried after the retrofit. This avoids drastic changes to the internal action distribution in the frame, at least in the range of the elastic behavior. Additionally, the chosen strength distribution of the dissipative braces aims at obtaining simultaneous yielding of the devices at all the stories and, thus, a global ductility of the bracing system coinciding with the ductility of the single braces. Given V^i_d and K^i_d, the braces properties (K^i_0, F^i_0 and K^i_b) at each story can be determined based on the number of braces and on geometrical considerations and applying Equation 2

3.2.2 Retrofit cases

In Figure 8a, the pushover curve obtained for the load distribution relative to the first vibration mode of the bare frame is shown and the limit corresponding to the failure of the most critical element, i.e., columns C1-2 of Figure 1, is posed in evidence. This limit corresponds to a strain demand ε_c in the most critical concrete fiber equal to the assumed capacity $\varepsilon_{cu}=0.0035$. The corresponding value of the top floor displacement is $d= 0.102$ m (which corresponds to a maximum inter-story drift of about 1.0%) and is assumed as design ultimate displacement (d_u) in the retrofit design methodology in order to limit damages on the bare frame elements. The corresponding base shear capacity is V^1_f =186 kN. In Figure 8b a picture of yielded and failed sections at this displacement level is given. Obviously, after this first failure, the bare frame has residual capacity up to a displacement of about $d= 0.18$ at which all the columns are failed at the base, as illustrated in Figure 8c. It is worth to notice that the damage distribution illustrated in Figure 8c is very similar to the damage layout experimentally observed under severe shaking and described in [8]. Failure of the beam-column joints as well the shear failure of the frame elements are not monitored in the pushover analysis, assuming that local retrofit measures will be applied to avoid these failure modes.

The bare frame is retrofitted by inserting a bracing system designed for several values of the ratio α between the base shear capacity of the bracing system V^1_d and that of the bare frame V^1_f in the range from 0.4 to 3.2. Elasto-plastic dissipative braces adopted for the case study described in this section are buckling-restrained braces. In particular, differently from buckling-restrained braced used in steel-structures, dissipative braces used in the case study are made by a buckling-restrained device placed in series with an elastic brace with adequate over-strength. In fact, when used in RC frame with low ductility which cannot undergo large displacements without failure, the device must be quite short so that they are able to yield for small displacements. An example of these devices may be found in [4]. Usually, the ductility capacity μ_{0u} of well detailed buckling-restrained devices is in the range 15-20 [46]. In this application the maximum ductility capacity of the devices is assumed equal to μ_{0u} = 15, while, in order to obtain adequate dimension of the elastic braces, the ductility capacity assumed for the dissipative brace is μ_{du}=12. In Figure 8a the pushover curves of the retrofitted frames are reported and compared with the pushover curve of the bare frame. In Table 3 the axial force F^i_d and the axial stiffness K^i_d of the dissipative braces are given for the different retrofit levels. From the properties of the dissipative braces, the properties of the buckling-restrained devices (K^i_0, F^i_0) and the stiffness of the elastic link braces (K^i_b) at each story can be determined based on indication given in the previous section. In the same table the vibration periods, calculated by considering an effective stiffness for the elastic part of the bare frame members, are also reported for each retrofit level.

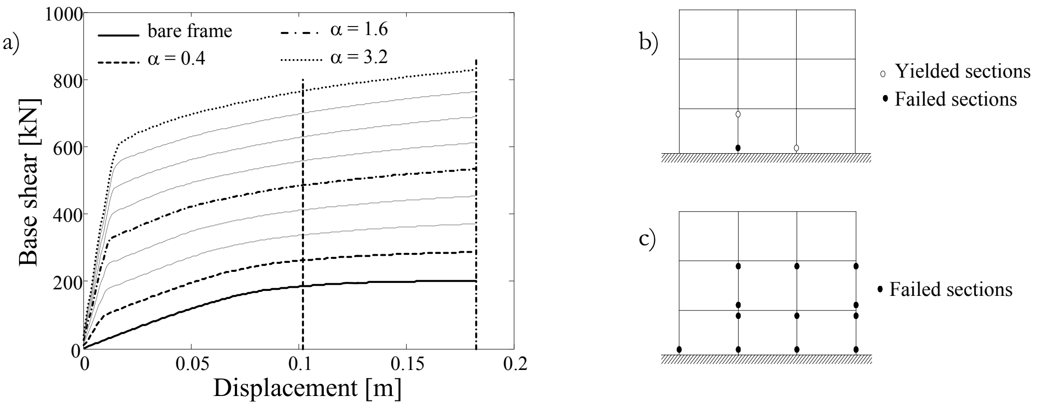

Figure 8. Pushover curves for bare and retrofitted frames.

Table 3. Braces properties at each story

	α=0.4		α =0.8		α =1.2		α =1.6	
T	0.670 sec		0.521 sec		0.448 sec		0.404 sec	
Story	F_d^i	K_d^i	F_d^i	K_d^i	F_d^i	K_d^i	F_d^i	K_d^i
	[kN]	[kN/m]	[kN]	[kN/m]	[kN]	[kN/m]	[kN]	[kN/m]
1	88	36046	175	72091	263	108137	351	144183
2	75	25106	150	50212	226	75317	301	100423
3	43	22921	86	45843	130	68764	173	91685
	α =2.0		α =2.4		α =2.8		α =3.2	
T	0.374 sec		0.352 sec		0.335 sec		0.321 sec	
Story	F_d^i	K_d^i	F_d^i	K_d^i	F_d^i	K_d^i	F_d^i	K_d^i
	[kN]	[kN/m]	[kN]	[kN/m]	[kN]	[kN/m]	[kN]	[kN/m]
1	438	180228	526	216274	614	252319	702	288365
2	376	125529	451	150635	526	175741	601	200847
3	216	114607	259	137528	302	160449	346	183371

3.2.3 Vulnerability assessment

For the purpose of developing fragility curves, a number of 30 natural g.m. records are selected from the European database [3]. These records are compatible with the uniform hazard spectrum type 1 given by the Eurocode 8 [18] with soil type D (S =1.35) and peak ground acceleration a_g=0.1Sg. They have been chosen in a range of magnitude and source to site distance of 5.5-7.0 and 25-75 km respectively. The spectral acceleration at the fundamental period of the structure S_a(T) is used as seismic intensity measure *IM*. Thus, the records are scaled so that they have the same IM, i.e. the same spectral acceleration at the fundamental period of the system. It is noteworthy that the vibration period and consequently the IM are different for the bare and the retrofitted frames and also vary with α.

In developing the fragility curves, the limits of the concrete and steel capacity are set equal to ε_{cu} = 0.0035 and ε_{su} = 0.04 [18]. The shear resistance of beams and columns and the resistance in tension and in compression of beam-column-joints are evaluated according to the formulas proposed by [40].

In Figure 9a the points of the numerical fragility of the bare frame and the fitted lognormal fragility curve are plotted. Figure 9a suggests that the lognormal curves fit very well the numerical fragility. Thus, only lognormal curves will be shown hereinafter. In Figure 9b fragility curves relevant to the different failure modalities considered are reported. The most significant failure mode is the failure of joints in tension while failure of joints in compression and shear failure have a zero probability of occurrence. However, in this study joint cracking is not considered as system failure mode and will be disregarded hereinafter in the development of the fragility curves. Consequently, concrete failure (*LS1*) becomes the most critical collapse modality, while steel failure (*LS2*) is much less probable.

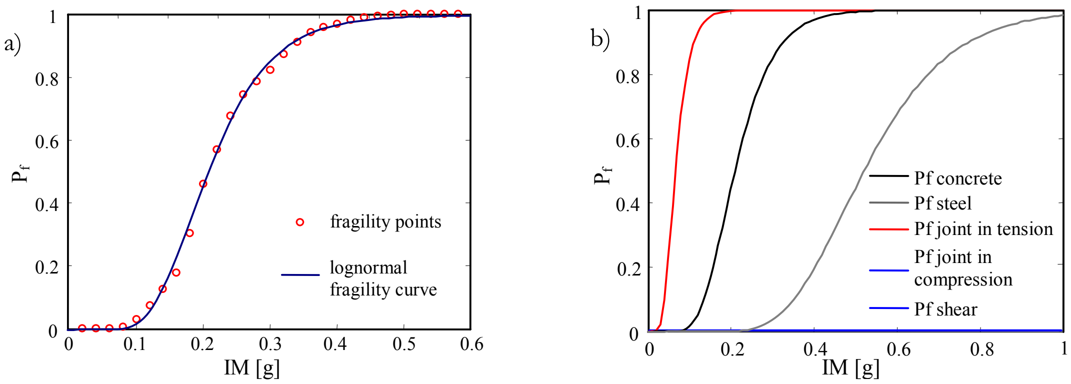

Figure 9. Fragility curves related to a) the system and b) the different failure modalities.

Figure 10 shows the fragility curve of the system and of the most vulnerable elements, for the bare frame and three retrofitted frames, corresponding to α=0.4, α=1.6 and α=3.2. Column *C1-2* and column *C1-3,* failing in concrete crushing mode (*LS1*), are the most vulnerable components before and after the retrofit, according to the results of the pushover analysis. However, for the bare frame as well for low values of α (α =0.4) the fragility curves of the two columns are very close to each other, thus vulnerability of the two system components is very similar. Differently, for increasing values of α (α=1.6 and α=3.2) the two curves are more spaced and the curve of the column C1-2 tends to coincide with the system fragility curves, thus the failure of the system is due to the C1-2 column failure in the 100% of cases. This is attributed to the fact that the placement of the bracing leads to a higher level of axial load to be resisted by column C1-2 when compared with column C1-3 and to the fact that the difference became higher for increasing value of the coefficient α. Furthermore, it should be observed that for all the levels of the retrofit considered, the fragility curve of the most vulnerable dissipative brace (i.e., *D1*) are close to the fragility curves of the most vulnerable elements of the frame. The comparable vulnerabilities of the frame components and of the dissipative devices confirm the reliability of the simplified design method, which aims at achieving a simultaneous failure of both the frame and the braces.

Figure 11a reports the system fragility curves of the bare frame and of the retrofitted frames, for all the different α values considered in the study. Obviously, an increase of $IM_{c,50}$ can be observed for increasing values of α, however this parameter does not directly provide information about the effectiveness of the retrofit, since the natural period of the systems are different. Figure 11b reports the variation with α of the factors m_{50}, m_{84}, and m_{16}, defined according to Section 3.2 which may be directly used to evaluate the effectiveness of the retrofit. It is observed that for low α values, an increase of α yield a significant increase of the collapse margin ratio, while for large values of α (higher than 1.5) the relation between the collapse margin ratios and α becomes strongly non linear and an increase of α does not yield a significant increase of the collapse margin ratio. This trend is consequence of the effect of axial force increment on the columns involved by the bracing systems and lead to the conclusion that the effectiveness of the retrofit system is strongly reduced for value of α larger than 1.5.

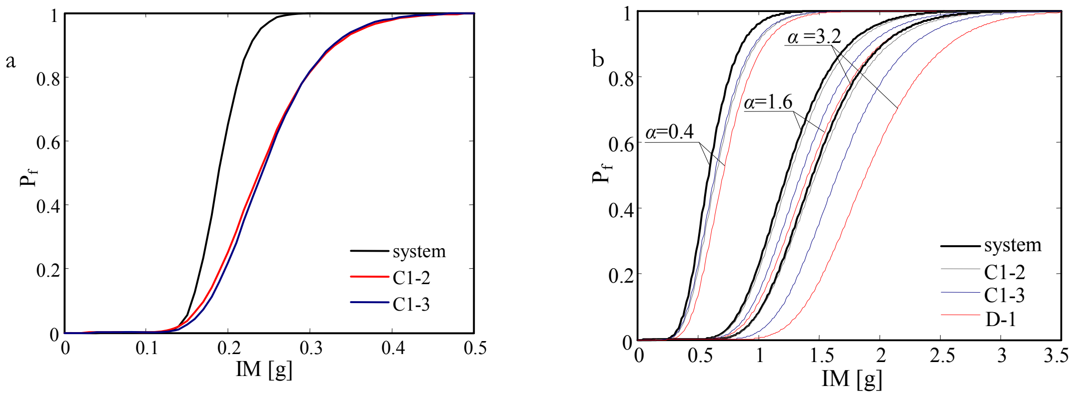

Figure 10. Fragility curve of the system and of the most vulnerable components for a) the bare frame and b) the frame retrofitted for selected α levels.

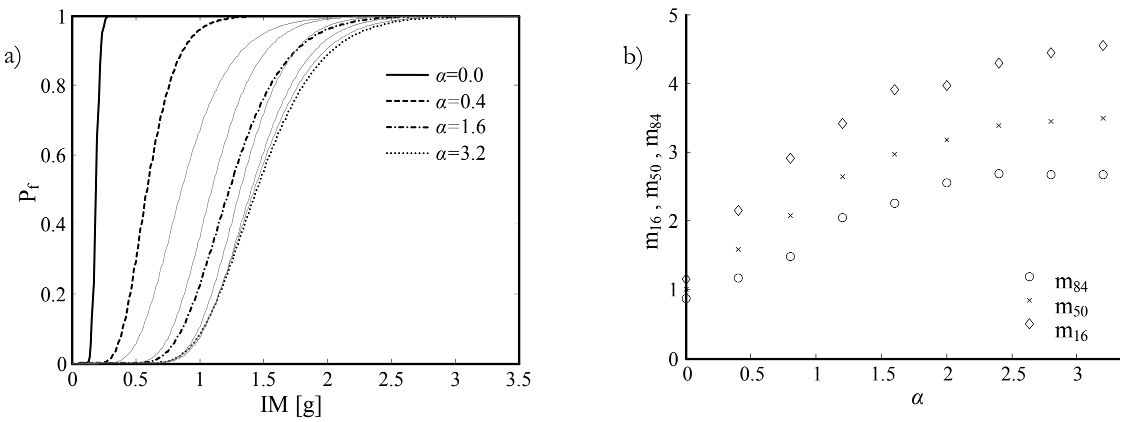

Figure 11. a) System fragility curves for the bare frame and for the retrofitted frame, and b) variation with v of the factors m_{50}, m_{84} and m_{16}.

Figure 12a plots the dispersion measure β_c evaluated according to Equation 1 for increasing values of α and shows that a significant increase of the dispersion occurs when elastoplastic braces are introduced into the bare frame. In fact, the value of β_c for all the cases of retrofit is significantly larger than the corresponding value of the bare frame. This can be explained recalling that the dissipative braces yield a more pronounced nonlinear behavior and this may add dispersion to the response when it is evaluated in terms of displacement. Furthermore, accounting for the vulnerability of the braces in addition to that of the frame components necessarily results in an increase of global dispersion of demand.

Finally, Figure 12a reports the comparison between the factor m_{50} and of the factors $m_{50,\theta}$ and $m_{50,TSD}$ obtained by elaborating fragilities curves developed by considering global EDPs, in particular the maximum inter-story drift (θ) and the top story drift (TSD), respectively. In order to make this comparison, global EDPs limits are chosen so that $IM_{c,50}$ =

$IM_{c,50;\,\theta}$ ($m_{50,\theta}$ =1) and $IM_{c,50} = IM_{c,50;TSD}$ ($m_{50,\mathrm{TSD}}$=1) for the case of bare frame. From Figure 12a is evident that, if the same value of the global EDP limit is assumed for the bare and the retrofitted frames, a significant overestimation of the seismic increment capacity of the retrofitted frames is obtained, especially for large values of the retrofit level. In fact, by using this strategy, local phenomena such as the increment of the axial force of the columns involved in the dissipative bracing system are not accounted for. In order to accurately estimate the efficiency of the retrofit based on dissipative braces, proper limits need to be estimate for each retrofit level, if global EDPs are considered, otherwise local EDP must be used.

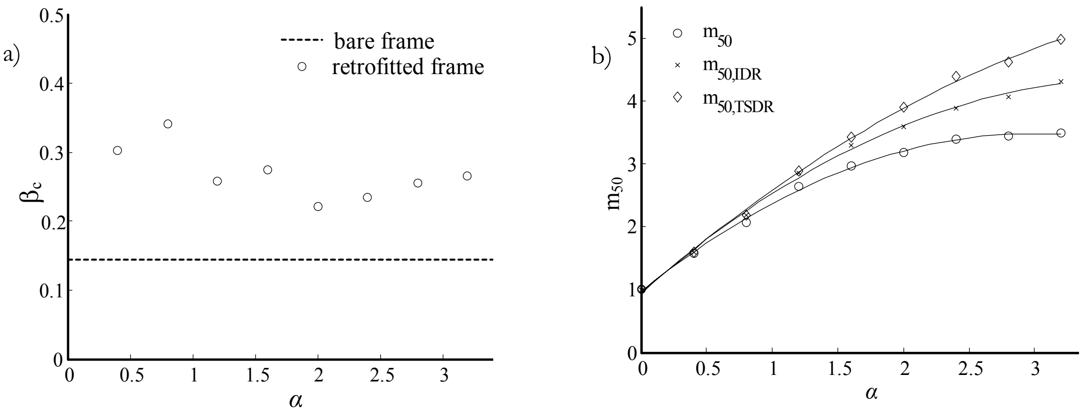

Figure 12. Variation with v of a) the factor m_{50} by considering different EDPs and b) the dispersion measure β_c

4 Conclusions

In the study, the use of local EDPs is provided in order to achieve a more accurate understanding of the seismic behavior of low ductility RC frames.
A first part of the work proposes a methodology for the probabilistic seismic demand analysis of low-ductility RC frame buildings, to support multi-component vulnerability assessment of such structures which exhibit susceptibility to damage under earthquake loads. In particular, this study considers local and global EDPs, explores the appropriate form of PSDM in terms of the regression model and analyzes the performance of alternative IMs on the basis of such criteria as model efficiency. Furthermore, uncertainty of the demand including probability distribution and homoscedasticity are tested. Among the traditional and advanced ground motion IMs, 14 structure dependent and structure independent IMs are assessed to identify IMs that "best" respect the requirements of practicality, sufficiency, hazard computability and efficiency. Twelve EDPs indicative of damage potential to RC buildings are considered that span the categories of local, intermediate, and global response quantities. To construct the PSDMs for all IM-EDP pairs and structural components, non linear dynamic analyses are conducted on the validated model using a set of 240 ground motions.

Optimal PSDMs confirm that linear regression (in the logarithmically transformed space) provides a good fit of the demand for conventionally used global EDPs, while it is found that for local and intermediate EDPs, such as curvature, shear, joint stresses, or material strains, a bilinear regression is required.

The sufficiency test of each IM with respect to magnitude and source to site distance indicates that among all considered IM-EDP pairs, PGA and $S_{a\text{-}02s}$ are insufficient with respect to magnitude, while PGD, I_v and CAD are found to be insufficient with respect to distance for most of the EDPs. PGV best satisfies the sufficiency hypothesis with respect to both distance and magnitude, while all other IMs were found to be equally sufficient. Assessment of the demand dispersions indicates that structure dependent IMs are much more efficient for all considered EDPs relative to the structure independent IMs, with approximately 50%-75% lower β_D. Among the structure independent IMs, PGV and $S_{a\text{-}1s}$ are the most efficient while $S_{a\text{-}02s}$ and PGA produce the largest values of dispersion. Among the structure dependent IMs, $S_a(T_1)$ and $S_d(T_1)$ have the lowest β_D, while $S_v(T_1)$, $S_{N1}(T_1)$ and $S_{aC}(T_1)$ are all relatively efficient.

The homoscedasticity assumption is evaluated for all of the PSDMs showing that for local and intermediate EDPs this condition is not satisfied, regardless of IM. Thus the variability of the dispersion should be taken into account when defining fragility curves of the RC building components. While structure independent IMs show improved conformance in terms of homoscedasticity for global EDPs, this outcome is an artifact of the poor efficiency and overall high dispersion in the models which is not ideal. Kolomogorov-Smirnov goodness-of-fit tests are conducted to investigate the validity of the typical assumption that the demand can be modeled by a lognormal probability distribution, revealing the superiority of the structural dependent IMs to satisfy this assumption. Overall, $S_d(T_1)$ and $S_a(T_1)$ are found to best satisfy the requirement of practicality, sufficiency, hazard computability and efficiency across the range of EDPs, while satisfying traditional lognormal probability distribution assumptions. Bilinear regressions with heteroscedastic dispersions are required in the PSDA for local and intermediate EDPs, regardless of IM selection.

The second part of the work illustrates a probabilistic methodology for assessing the vulnerability of existing RC buildings with limited ductility capacity and retrofitted by means of dissipative braces. The methodology is based on the development of fragility curves of the bare and the retrofitted frame. It employs non linear incremental dynamic analysis under a set of input ground motions to account for the randomness of the earthquake excitation and local EDPs to capture the modifications of the frame response induced by the introduction of the bracing system. Furthermore, in addition to global system fragility curves, component fragility curves are built for single structural components, in order to monitor the most vulnerable elements before and after the retrofit. The methodology developed allows to evaluate the safety level reached by the frame before and after the retrofit by taking into account the probabilistic properties of the seismic response and at the same time, employing an efficient structure dependent IM. The methodology can be also used to evaluate the effectiveness of the criterion employed to design the dissipative braces.

The proposed methodology is applied in this study to a benchmark RC frame with limited ductility capacity and retrofitted by elasto-plastic braces for different values of the shear capacity of the bracing system. The comparable vulnerabilities of the frame and of the dissipative braces obtained for the various retrofit levels confirm the effectiveness of the simplified criterion often employed to design the braces, which aims to achieve a simultaneous failure of both the frame and the braces. For large values of the retrofit levels the most loaded column involved in the dissipative bracing system becomes a very vulnerable element of the system. This is consequence of the effect of axial force increment on the columns involved by the bracing systems, the obtained results show that, for low α values, the seismic capacity significantly increases for increasing values of α, while for large values of α (higher than 1.5) the relation an increase of α does not yield a significant increase of seismic capacity of the frame. By performing similar evaluation by using overall maximum interstory drift and top story drift, the increase of seismic capacity is overestimated highlighting the lack of accuracy linked to the use of these global EDPs. Finally, an increase of the dispersion of the retrofitted frames with respect to the bare frame is shows. This can be explained by recalling that the dissipative braces yield a more pronounced non linear behavior and this may add dispersion to the response when it is evaluated in terms of displacements. This result implies the importance of considering the dispersion in the evaluation of seismic safety level achieved after the retrofit.

References

[1] ACI Committee 318. Building code requirements for reinforced concrete and commentary (ACI 318-89/ACI 318-R89), American Concrete Institute, Detroit 1989.

[2] Aycardi, L. E., Mander, J. B., Reinhorn, A. M., 1992. Seismic Resistance of Reinforced Concrete Frame Structures Designed Only for Gravity Loads - Part II: Experimental Performance of Subassemblages, NCEER Report.

[3] Ambraseys N, Smith P, Berardi R, Rinaldis D, Cotton F, Berge-Thierry C. Dissemination of European Strong-Motion Data. CD-ROM Collection. European Council, Environment and Climate Research Programme, 2000.

[4] Antonucci R, Balducci F, Castellano M G, Donà F. Pre-casted RC buildings with buckling restrained braces: the example of the new building of the faculty of engineering in Ancona,. *Proceedings of 2nd International FIB Congress*, Napoli, 2006.

[5] Bai, J.W., Gardoni, P., et al., 2011. Story-specific demand models and seismic fragility estimates for multi-story buildings, *Structural Safety* **33**, 96-107.

[6] Baker, J., et al., 2011. Ground Motion Studies for Transportation Systems, *PEER Website*, (http://peer.berkeley.edu/transportation/projects/ground-motion-studies-for-transportation-systems/)

[7] Bracci, J. M., Reinhorn, A. M., Mander, J. B., 1992a. Seismic Resistance of Reinforced Concrete Frames Structures Designed only for Gravity Loads: Part I, NCEER Report.

[8] Bracci, J. M., Reinhorn, A. M., Mander, J. B., 1992b. Seismic Resistance of Reinforced Concrete Frame Structures Designed Only for Gravity Loads-Part III: Exp Performance and Analytical Study of a Model, NCEER Report.

[9] Bradley, B.A., and Dhakal, R.P., 2008, "Error estimation of closed form solution for annual rate of structural collapse", *Earthquake Engineering and Structural Dynamics, 37:1721-1737.*

[10] Christopoulos C, Filiatrault A. *Principles of passive supplemental damping and seismic isolation.* IUSS Press: Pavia, Italy, 2006.

[11] Conover, W.J., 1999, "Practical Nonparametric Statistical.", John WIley & Sons, Inc. New York, 3rd edistion.

[12] Cordova, P.P., Deierlein, G.G., Mehnnay, S.S.F., and Cornell, C.A., 2000. Development of a two-parameter seismic intensity measure and probabilistic assessment procedure, Proceding of the 2nd US-Japan workshop on performance-based earthquake engineering for reinforced concrete building structures.

[13] Cornell, C. A., and Krawinkler, H., 2000. Progress and challenges in seismic performance assessment, PEER Center News **3**(2).

[14] Cornell, C. A., Jalayer, F., et al., 2002. Probabilistic Basis for 2000 SAC Federal Emergency Management Agency Steel Moment Frame Guidelines, Journal of Structural Engineering **128**(4), 526-533.

[15] Dall'Asta, A., Ragni, L., Tubaldi, E., Freddi, F., 2009. Design methods for existing r.c. frames equipped with elasto-plastic or viscoelastic dissipative braces, XIII Convegno Nazionale

ANIDIS: L'Ingegneria sismica in Italia, Bologna, Italy.
[16] Di Sarno L, Manfredi G. Seismic retrofitting with buckling restrained braces: Application to an existing non-ductile RC framed building. *Soil Dynamics and Earthquake Engineering* 2010; 30(11): 1279-1297.
[17] El-Attar., A. G., White, R. N., et al., 1991. Shake table test of a 1/8 scale three-story reinforced concrete frame building designed primarily for gravity loads, Proceedings of the Canadian Conference on Earthquake Engineering, 639-639.
[18] European Committee for Standardization (ECS). Eurocode 8 - Design of structures for earthquake resistance, EN1998, Brussels, 2005.
[19] FEMA 356, 2000. Prestandard and Commentary for the Seismic Rehabilitation of Buildings, Federal Emergency Management Agency, Washington DC.
[20] Ghosh, J., and Padgett, J. E., 2011. Probabilistic seismic loss assessment of aging bridges using a component-level cost estimation approach. *Earthquake Engineering & Structural Dynamics.*
[21] Giovenale, P., Cornell, C.A., and Esteva, L., 2004. Comparing the adequacy of alternative ground motion intensity measures for the estimation of structural responses. *Earthquake Engineering and Structural Dynamics* **33**,951– 79.
[22] Güneyisi E M, Altay G. Seismic fragility assessment of effectiveness of viscous dampers in R/C buildings under scenario earthquakes. *Structural Safety* 2008; 30(5), 461-480.
[23] Guneyisi E M. Seismic reliability of steel moment resisting framed buildings retrofitted with buckling restrained braces. *Earthquake Engineering and Structural Dynamics* 2011.
[24] Hines, W., Montgomery, D., Goldsman, D., Borror, C., 2003. Probability and Statistic in Engineering. Wiley, New York.
[25] Hueste M D, Bai J W. Seismic Retrofit of a Reinforced Concrete Flat-Slab Structure: Part II Seismic Fragility Analysis. *Engineering Structures* 2006; 29(6), 1178-1188.
[26] Kasai K, Fu Y, Watanabe, A. Passive control systems for seismic damage mitigation. *Journal of Structural Engineering* 1998; 124(5): 501-512.
[27] Lee T H, Mosalam K M. Seismic demand sensitivity of reinforced concrete shear-wall building using FOSM method. *Earthquake Engineering and Structural Dynamics* 2005; 34(14), 1719-1736.
[28] Liel A B, Haselton C B, Deierlein G G. Seismic Collapse Safety of Reinforced Concrete Buildings: II. Comparative Assessment of Non-Ductile and Ductile Moment Frames, Journal of Structural Engineering 2011;137(4):492-502.
[29] Lin, L., Naumoski, N., et al., 2011. Improved intensity measures for probabilistic seismic demand analysis. part 1: Development of improved intensity measures, Canadian Journal of Civil Engineering **38**, 79-88.
[30] Luco, N., and Cornell, C. A., 2007. Structure-specific scalar intensity measures for near-source and ordinary earthquake ground motions, *Earthquake Spectra* **23**, 357-392.
[31] Lupoi G, Lupoi A, Pinto P E. Seismic risk assessment of rc structures with the "2000 sac/fema" method. *Journal of Earthquake Engineering* 2002; 6(4):499-512.
[32] Makie, K., and Stojadinovic, B., 2003. Seismic Demands for Performance-BasedDesign of Bridges, *PEER Report No. 13.*
[33] McKenna, F., Fenves, G. L., Scott, M. H., 2006. OpenSees: Open system for earthquake engineering simulation, Pacific Earthquake Engineering Center, University of California, Berkeley, CA.
[34] Moehle, J., and Deierlein, G. G., 2004. A Framework mothodologyfor performance-based earthquake engineering, 13th World Conference on earthquake Engineering, Vancuver, B.C., Canada.
[35] Özel A E, Güneyisi E M. Effects of eccentric steel bracing systems on seismic fragility curves of mid-rise r/c buildings: a case study. *Journal of Structural Safety* 2011; 33(1): 82-95.
[36] Padgett, J. E., Nielson, B. G., et al., 2008. Selection of optimal intensity measures in probabilistic seismic demand models of highway bridge portfolios, *Earthquake Engineering and Structural Dynamics* **37**, 711-725.

[37] Padgett J E, Des Roches R. Methodology for the development of analytical fragility curves for retrofitted bridges. *Earthquake Engineering and Structural Dynamics* 2008; 37:1157–1174.

[38] Panagiotakos, T. B., and Fardis, M. N., 2001. Deformations of reinforced concrete members at yielding and ultimate, ACI Structural Journal **98**, 135-148.

[39] Porter K A, Kiremidjian A S, Le Grue J S. Assembly-based vulnerability of buildings and its use in performance evaluation. *Earthquake Spectra* 2001; 17(2):291-312.

[40] Priestley, M.J.N., 1997, "Displacement-based seismic assessment of reinforced concrete buildings." *Journal of Earthquake Engineering.* 1(1):157-192..

[41] Ramamoorthy S, Gardoni, P, Bracci, J. Probabilistic Demand Models and Fragility Curves for Reinforced Concrete Frames. *Journal of structural Engineering* 2006;132(10):1563-1572.

[42] Scott, M. H., and Fenves, G. L., 2006. Plastic hinge integration methods for force-based beam-column elements, Journal of Structural Engineering **132**, 244-252

[43] Shome, N., 1999. Probabilistic Seismic Demand Analysis of Nonlinear structures, *Doctoral Dissertation*, Stanford University, Stanford, CA.

[44] Soong, T.T. and Spencer, B.F. Supplemental energy dissipation: state-of-the-art and state-of-the-practice. *Engineering Structures* 2002; 24(3); 243-259.

[45] Tubaldi E, Barbato M, Dall'Asta A. Influence of model parameter uncertainty on seismic transverse response and vulnerability of steel-concrete composite bridges with dual load path. *Journal of Structural Engineering* 2011.

[46] Uang C M, Nakashima M. Steel Buckling- Restrained Braced Frames. Chapter 16 of Earthquake Engineering, from Engineering Seismology to Performance-Based Engineering. CRC Press, 2004.

[47] Vamvatsikos D, Cornell C A. Incremental dynamic analysis. Earthquake Engineering and Structural Dynamics 2002; 31(3): 491-514.